UC Berkeley
UC Berkeley Previously Published Works

Title
Flow loss in superplasticized limestone calcined clay cement

Permalink
https://escholarship.org/uc/item/25f161rx

Authors
Moghul, Sirajuddin
Zunino, Franco
Flatt, Robert J

Publication Date
2024

DOI
10.1111/jace.20344

Copyright Information
This work is made available under the terms of a Creative Commons Attribution License, available at https://creativecommons.org/licenses/by/4.0/

Peer reviewed

eScholarship.org Powered by the California Digital Library
University of California

Check for updates

Received: 10 October 2024 | Revised: 20 November 2024 | Accepted: 3 December 2024

DOI: 10.1111/jace.20344

Journal of the American Ceramic Society

RESEARCH ARTICLE

Flow loss in superplasticized limestone calcined clay cement

Sirajuddin Moghul | **Franco Zunino** | **Robert J. Flatt**

Institute for Building Materials, ETH Zurich, Zurich, Switzerland

Correspondence
Robert J. Flatt, Institute for Building Materials, ETH Zurich, Switzerland.
Email: flattr@ethz.ch

Present address
Franco Zunino, Department of Civil and Environmental Engineering, University of California, Berkeley, USA

Funding information
Swiss National Science Foundation (SNF), Grant/Award Numbers: 172481, 208719; Schweizerischer Nationalfonds zur Förderung der Wissenschaftlichen Forschung, Grant/Award Number: 172481

Abstract

This study investigates the mechanisms behind fluidity loss in superplasticized limestone calcined clay cement (LC3), a sustainable alternative to ordinary Portland cement (OPC). Despite its environmental benefits, in presence of superplasticizers, LC3 experiences significant challenges in maintaining workability, an issue of which this paper examines the root cause. It focuses on the role that initial reactions play in creating additional surface area and the consequence thereof on the performance of polycarboxylate ether superplasticizers (PCE) in LC3. Experimental results reveal that while PCEs initially disperse the cement particles, fluidity decreases rapidly over time, primarily due to the continuous generation of those new surfaces that exceed the adsorption capacity of PCEs. The study also examines the potential intercalation of PCE side chains into calcined clays and shows that even in the worst-case scenario with montmorillonite clays, intercalation is not a significant contributor to slump loss when the clays are calcined. These findings suggest that alternative strategies, such as slowing down the initial reactivity of the calcined clays, for example by combining PCEs with other additives like diphosphonates, may be necessary to improve flow retention in superplasticized LC3 systems.

KEYWORDS
adsorption, flow loss, limestone calcined clay cement, specific surface area, superplasticizer

1 | INTRODUCTION

As the global effort to mitigate climate change intensifies, industries are under increasing pressure to innovate and reduce carbon emissions. The cement industry, responsible for nearly 8% of global CO_2 emissions, has become a key focus for sustainability efforts.[1] Ordinary Portland cement (OPC), the most widely used cement, is highly carbon-intensive, which has driven the development of alternative materials aimed at reducing the environmental impact of construction.[2] Among these alternatives, limestone calcined clay cement (LC3), has shown substantial promise.[3,4] In LC3 cements, a portion of OPC is substituted with calcined clay and limestone—two materials that are abundant, cost-effective, and environmentally less impactful.[5,6] By incorporating these components, LC3 can reduce CO_2 emissions by up to 30–40% compared to traditional OPC when a 50% replacement level of OPC is used, offering equivalent mechanical properties and enhancing durability, and with the potential to go even higher in replacement for general use applications. This positions LC3 technology as a viable solution for sustainable cement production.[7–9]

This is an open access article under the terms of the Creative Commons Attribution License, which permits use, distribution and reproduction in any medium, provided the original work is properly cited.
© 2024 The Author(s). Journal of the American Ceramic Society published by Wiley Periodicals LLC on behalf of American Ceramic Society.

Despite its environmental benefits, LC3 faces a critical obstacle that challenges its wider adoption in the construction industry: its inability to retain slump in presence of the most widely used type of superplasticizers, leading to a rapid loss of fluidity in fresh concrete. This loss of fluidity complicates the handling, transportation, placement, and finishing of concrete, thereby impacting workability.[10–14] Given the operational challenges and potential effects on construction efficiency, understanding the factors that contribute to slump loss in superplasticized LC3 is essential for improving its performance and facilitating its broader use in demanding practical applications.

The literature identifies three primary reasons behind LC3's poor slump retention: (1) the adsorption of water by calcined clay, (2) the potential intercalation of PCEs with calcined clay, and (3) the high specific surface area (SSA) of calcined clay.[10,15–17] Initially, the water adsorption capacity of calcined clay was thought to reduce free water in the mix, reducing fluidity.[15] However, recent studies, such as those by Luca et al., have shown that water adsorption is not the primary cause of slump loss in LC3.[18] This shifts the focus to other potential mechanisms, particularly the interaction between calcined clay and PCEs, as well as the large SSA of calcined clay.

PCEs, a widely used class of superplasticizers, have proven highly effective in enhancing workability and maintaining slump retention in OPC systems, even when limestone is used as a filler or supplementary replacement material.[14,19–21] However, in LC3, which contains calcined clays alongside OPC and limestone, PCEs do not provide the same level of performance. This suggests that calcined clay is a key driver of slump loss in LC3. The high SSA of calcined clay is considered a major contributor to this issue, as it increases water demand and makes it more difficult to maintain fluidity.[10,16] In theory, higher dosages of PCEs used for LC3 should offset this effect by adsorbing onto all particles, preventing flocculation, promoting better dispersion, and improving slump retention. Yet, despite the higher dosages of superplasticizers in LC3 formulations, which initially provide good dispersion (hence adequate initial slump) typically on the order of 20–30 min, rapid slump loss persists.[14] It should also be noted that higher dosages ultimately may also lead to the bleeding depending on the liquid to solid ratio used.

The fast flow loss even at high dosages raises an intriguing question: if higher dosages of PCEs are theoretically sufficient to counteract the increased water demand due to the high SSA of calcined clay and offer initial fluidity, why does fluidity continue to decrease so rapidly? As the issue continues, the potential for PCE intercalation with calcined clay has also been explored as a possible contributing factor. Indeed, in calcined clays, unlike swelling clays where PCE intercalation is a well-established cause for poor fluidity.[22–24] Thus, the interaction between PCEs and calcined clays remains unclear and warrants further investigation. The fact that PCEs provide initial dispersion but fail to retain fluidity may suggest that other mechanisms may be at play, particularly related to the calcined clay's behavior in the mix.

The yield stress of suspensions can be assessed considering the number of contacts between grains and the cohesiveness of those contacts,[25] a concept that has recently also been shown to account for thixotropic build up at rest.[26] In presence of superplasticizers, a weighted average force can be computed considering the number of contacts where both opposing surfaces are either devoid of adsorbed polymers, both containing adsorbed polymers, or having one surface with and one without polymers.[27] It can be shown that up to high surface coverages, the contacts devoid of polymers dominate this force, which implies that if hydrates are being produced at contact points between grains, they can have an important effect in increasing the overall cohesiveness of the flocculated network and therefore the yield stress.[28] Similarly, because the adsorption of PCEs is reversible, they may be displaced toward newly formed hydrates for which they may have a stronger affinity, leaving the intergranular contacts to become much more cohesive. Such effects are expected to be strongly affected by any change in SSA caused by the precipitation of hydrates. The focus of this paper is therefore to examine to what extent such changes in SSA may account for flow loss in LC3.

By addressing these factors, this research seeks to provide a clearer understanding of the challenges facing superplasticized LC3 in maintaining workability and to offer insights that could lead to the development of improved formulations with enhanced slump retention properties. Resolving these issues is critical for the successful adoption of LC3 as a sustainable alternative to OPC, thereby supporting global efforts to reduce carbon emissions in the construction industry and combat climate change.

2 | MATERIALS, METHODOLOGY, AND METHODS

2.1 | Materials

In this study, ordinary Portland cement (CEM I 42.5R) from the Holcim Group, compliant with EN 197-1 standards, and limestone (LS) from Betocarb HP, OMYA,

15512916, 0, Downloaded from https://ceramics.onlinelibrary.wiley.com/doi/10.1111/jace.20344 by Univ of California Lawrence Berkeley National Lab, Wiley Online Library on [29/01/2025]. See the Terms and Conditions (https://onlinelibrary.wiley.com/terms-and-conditions) on Wiley Online Library for rules of use; OA articles are governed by the applicable Creative Commons License

TABLE 1 Molecular parameters of used polycarboxylate ether superplasticizers (PCE).

Molecular Parameters	Values
Solid content (wt%)	52
Backbone	PMAA-4900 g/mol
Sidechain	MPEG-3000 g/mol
C/E	5
Mw (g/mol)	54 600
PDI (Đ)	2.3
Amount of carboxyl groups per unit mass of the PCE (mmol/g) according to Mw	0.76
Number of monomers per side chain (P)	66
Number of monomers in the backbone from one side chain to another (N)	6
Number of repeating structural units (n)	15.92
Gay and Raphaël conformation type	FBW

Abbreviations: FWB, flexible backbone worm; MPEG, methoxy polyethylene glycol; Mw, molecular weights; PDI, polydispersity indices; PMAA, poly(methacrylic acid).

were used to produce LC3 blends. The third essential component, raw and calcined clays, was sourced from different suppliers. Kaolinitic raw clay (KRC) was obtained as a sample of raw feed of an industrial pigment quality high-purity metakaolin, and montmorillonite raw clay (MRC) was sourced from Fisher Scientific. Additionally, Holcim provided the industrially flash-calcined clay (ICC), while both raw clays were calcined in a laboratory muffle furnace at 800°C for 1 h, resulting in kaolinitic calcined clay (KCC) and montmorillonite calcined clay (MCC).[29]

Five types of LC3 cements were produced: IC-LC3, using the industrial calcined clay; KC-LC3, incorporating kaolinitic calcined clay; MC-LC3, using montmorillonite calcined clay; and KR-LC3 and MR-LC3, incorporating raw kaolinitic and montmorillonite clays, respectively. Each LC3 cement followed the most used LC3 50 formulations, consisting of 53.5% OPC, 15% limestone, 30% calcined clay, and 1.5% gypsum by mass. The gypsum content of IC-LC3 was first determined through preliminary isothermal calorimetry tests to ensure sufficient sulfation, specifically targeting the aluminate peak between 2 and 4 hours after the alite peak.[30] To maintain consistency and minimize variations in ettringite precipitation, the same gypsum content was used across all cement types.

PCE used in the study was a non-commercial lab product provided by Sika, with molecular parameters detailed in Table 1. Cement pastes were prepared using a vertical stirrer with a 45 mm diameter, 4-bladed propeller at a mixing speed of 1600 rpm. To control the temperature, the beaker containing the paste was immediately placed in a water bath at 20°C after mixing, ensuring that hydration proceeded similarly to the samples in the calorimeter. The chemical composition and physical properties of the materials and cements are presented in Table 2 and 3, respectively. Methoxy polyethylene glycol (MPEG) side chains of 1000 g/mol, also sourced from Sika, were used to study adsorption on OPC, limestone, and LC3 systems. Additional chemicals needed for the model system—including calcium hydroxide, calcium sulfate, potassium hydroxide, and sodium hydroxide—were sourced from Sigma-Aldrich. The model system's alkaline solution was composed of 0.1 mol/L sodium hydroxide and 0.5 mol/L potassium hydroxide. A summary of the important abbreviations used in the study is provided in Table 4 to make the reader familiar with them.

2.2 | Methodology

This study is divided into three main parts, each focusing on different aspects of the interaction between calcined clays, hydration reactions, and polymer adsorption in LC3 systems.

The first part of the study focused on the adsorption of PCE side chains on different LC3 cements prepared from raw and calcined clays. Since OPC and limestone are key components of LC3, their adsorption characteristics were also examined to provide a more comprehensive understanding of the entire system. To achieve this, a water-to-solid ratio of 0.5 was selected for all the materials, except for the LC3 with raw montmorillonite (MR-LC3), which required a higher water-to-solid ratio of 1 due to its higher water demand. Additionally, a fixed dosage of side chains, corresponding to 0.5% by weight of solids, was selected uniformly for all materials. Total organic carbon (TOC) analysis was used to study the adsorption behavior of PCE side chains on OPC, limestone and different LC3 cements providing insights into how surface characteristics and clay type affect polymer-clay interactions in LC3 systems. Additionally, for the LC3 with calcined montmorillonite, adsorption over time was also analyzed to determine if it could regain its intercalation capability. Adsorption is typically determined by measuring the depletion of organic carbon from solution using TOC measurements, allowing for the quantification of polymer adsorption onto different surfaces.[31–33]

The second part aimed to investigate whether calcined clays take part in initial hydration reactions. For this purpose, two LC3 systems prepared from raw clay and calcined clay produced in the laboratory from the same clay were

15512916, 0, Downloaded from https://ceramics.onlinelibrary.wiley.com/doi/10.1111/jace.20344 by Univ of California Lawrence Berkeley National Lab, Wiley Online Library on [29/01/2025]. See the Terms and Conditions (https://onlinelibrary.wiley.com/terms-and-conditions) on Wiley Online Library for rules of use; OA articles are governed by the applicable Creative Commons License

TABLE 2 Chemical composition and physical properties of the materials.

Properties		OPC	LS	ICC	KRC	KCC	MRC	MCC
Chemical Composition (wt%)	CaO	64.92	55.53	0.48	0.01	0.01	1.55	1.97
	SiO_2	21.01	0.34	63.00	45.19	52.25	49.48	62.74
	Al_2O_3	5.03	0.06	25.26	38.76	44.73	15.52	19.68
	Fe_2O_3	3.43	0.04	6.08	0.42	0.48	3.78	4.80
	MgO	1.94	0.25	0.49	0.02	0.02	2.23	2.83
	Na_2O	0.18	0.00	0.13	0.20	0.24	1.89	2.40
	K_2O	0.99	0.01	1.95	0.29	0.33	0.41	0.52
	Minor oxides	0.62	0.01	0.76	1.15	1.33	1.33	1.69
	LOI	1.88	43.75	1.84	13.97	0.62	23.80	3.38
Physical properties	Specific gravity	3.12	2.76	2.66	2.61	2.58	2.69	2.54
	SSA (m^2/g)	0.81	0.98	25.6	12.61	12.07	13.61	5.73
	D10 (μm)	6.71	5.51	1.99	4.61	5.40	1.31	9.05
	D50 (μm)	15.55	17.08	10.35	9.40	10.33	6.58	29.59
	D90 (μm)	42.06	52.73	55.39	17.11	21.87	55.19	86.68
	Dm (μm)	20.68	24.24	21.32	10.36	16.58	19.28	41.36

Abbreviations: ICC, industrially flash-calcined clay; KCC, kaolinitic calcined clay; KRC, kaolinitic raw clay; MCC, montmorillonite calcined clay; MRC, montmorillonite raw clay; OPC, ordinary Portland cement.

TABLE 3 Chemical composition and physical properties of different LC3 cements.

Properties		IC-LC3	KR-LC3	KC-LC3	MR-LC3	MC-LC3
Chemical Composition (wt%)	CaO	44.18	44.03	44.03	44.50	44.62
	SiO_2	30.51	25.16	27.28	26.45	30.43
	Al_2O_3	10.35	14.40	16.19	7.43	8.68
	Fe_2O_3	3.72	2.02	2.04	3.03	3.33
	MgO	1.25	1.11	1.11	1.78	1.96
	Na_2O	0.14	0.16	0.17	0.67	0.82
	K_2O	1.13	0.64	0.65	0.67	0.70
	Minor oxides	0.57	0.69	0.74	0.74	0.85
	LOI	8.15	11.79	7.78	14.74	8.61
Physical properties	Specific gravity	2.93	2.91	2.90	2.94	2.89
	SSA (m^2/g)	8.36	4.37	4.23	6.62	2.28
	D10 (μm)	5.54	5.45	6.00	7.09	7.36
	D50 (μm)	14.42	11.48	13.91	16.83	19.54
	D90 (μm)	50.46	33.85	53.89	51.29	65.02
	Dm (μm)	22.21	16.71	23.07	23.95	30.29

selected. This ensured that both systems had a similar filler effect, with differences attributed only to the chemical reactivity of the clays rather than their SSA. A water-to-binder ratio of 0.5 was adopted. Isothermal calorimetry was used to monitor heat evolution during hydration, while SSA measurements were conducted by stopping hydration at regular intervals during the first hour, with measurements conducted immediately after mixing and at every 15 minutes. Additionally, a model system developed by Scherb et al. was used to further investigate the role of calcined clays in the hydration process.[34]

The third part of the study is focused on tracking the evolution of SSA and the adsorption of PCE over time in two systems: OPC and LC3, both having the same initial yield stress. A water-to-binder ratio of 0.35, with PCE dosages of 0.12% and 0.35% by weight of the binder for OPC and LC3, respectively was used. These dosages ensured that both systems achieved an initial yield stress of 2 Pa,

15512916, 0, Downloaded from https://ceramics.onlinelibrary.wiley.com/doi/10.1111/jace.20344 by Univ of California Lawrence Berkeley National Lab, Wiley Online Library on [29/01/2025]. See the Terms and Conditions (https://onlinelibrary.wiley.com/terms-and-conditions) on Wiley Online Library for rules of use; OA articles are governed by the applicable Creative Commons License

TABLE 4 Summary of abbreviations used in the study.

Abbreviation	Full form
KRC	Kaolinitic raw clay
KCC	Kaolinitic calcined clay
KR-LC3	LC3 prepared from kaolinitic raw clay
KC-LC3	LC3 prepared from kaolinitic calcined clay
MRC	Montmorillonite raw clay
MCC	Montmorillonite calcined clay
MR-LC3	LC3 prepared from montmorillonite raw clay
MC-LC3	LC3 prepared from montmorillonite calcined clay
IC-LC3	LC3 prepared from industrially calcined clay
OPC-NFLC	OPC with no flow loss compensation
IC-LC3-NFLC	IC-LC3 with no flow loss compensation
IC-LC3-FLC	IC-LC3 with flow loss compensation

as determined using the mini slump cone and converting the diameter of the slump cone to yield stress.[35] In both instances, PCE was added directly to the mixing water. These experimental conditions, aligned with previous studies, ensured comparability and enabled accurate interpretation of the results. Similar to the second part, SSA measurements were conducted at 15-minutes intervals during the first hour to monitor changes over time, while TOC analysis was performed simultaneously to assess PCE adsorption. In a separate experiment, PCE was added at intervals to compensate the flow loss of IC-LC3, with corresponding TOC analyses conducted to track polymer adsorption. The total additional PCE required to compensate for the flow loss of IC-LC3 was 0.08% by weight of binder. Figure 1 shows the schematic representation of the experimental setup. It is important to note that the clays used in this part differed from the clays in the other two parts, as the raw version of the industrially calcined clay used later was not available.

2.3 | Methods

2.3.1 | Calorimetry

Since capturing the initial heat flow (within the first hour) is important for understanding the role of calcined clays in early hydration reactions, all calorimeter experiments were conducted using insitu mixing. The cement hydration experiments were carried out at 20°C, while the model cement experiments were performed at 25°C (as recommended by Scherb et al.[34]). All the samples were preconditioned to the temperature of the calorimeter for a day in a climatic chamber.

2.3.2 | Specific surface area measurements

To study the evolution of the SSA of cements during the first hour of hydration, solvent exchange was used to stop hydration immediately after mixing (at 2 minutes) and at 15-minute intervals over one hour. Freshly mixed paste (2 g) was diluted with cold isopropanol (IPA, Sigma-Aldrich, puriss. p.a., ACS reagent > 99.8%) in a 10:1 isopropanol-to-paste ratio.

Conventionally, the diluted paste is filtered using nylon membranes (0.22 or 0.45 μm), and then the moist paste is dried in a desiccator until a constant mass is achieved before measuring SSA using BET analysis.[25,36,37] However, as Sha et al. pointed out, this method can lead to the loss of nuclei and small ettringite crystals through the filter pores, especially with high superplasticizer dosages, causing an underestimation of SSA.[37] This occurs because the adsorption of superplasticizer onto ettringite crystals can inhibit crystal growth and drastically reduce the size of the ettringite crystals.[38]

To address this issue, after adding cold isopropanol to the paste, the slurry was centrifuged at 20,000 rpm for 8 h using a high-speed centrifuge (Beckman Coulter Allegra 64R). The centrifugation duration was calculated to sediment all particles larger than one nanometer.[39] After centrifugation, the supernatant was discarded, and the centrifuge tubes with samples were dried for 3 days in a climate-controlled chamber at 40°C under nitrogen purge to maintain an inert atmosphere. These conditions were selected to prevent the decomposition of ettringite.[36] Once dry, the samples were recovered from centrifuged tubes and homogenized in an agate mortar for BET SSA measurement.

The homogenized samples were degassed for 16 hours at 40°C in a VacPrep 061 degassing station (Micromeritics) under a nitrogen flow rate of 3×10^{-3} m^3/h. SSA was then determined using a BET multi-point nitrogen physisorption apparatus (Micromeritics Tristar II 3020) with an 11-point isotherm measured at 77 K and relative pressures (P/P_0) ranging from 0.05 to 0.30.[36]

2.3.3 | Adsorption studies

Two separate adsorption experiments were carried out: one focused on the adsorption of side chains onto various surfaces, such as OPC, limestone, and different types of LC3 cements, while the other examined the adsorption of PCE on IC-LC3. In the side chains adsorption experiment, side chains were added and dissolved in the mixing water, following the same approach as the direct addition of superplasticizer used in the study. The surface was

15512916, 0, Downloaded from https://ceramics.onlinelibrary.wiley.com/doi/10.1111/jace.20344 by Univ of California Lawrence Berkeley National Lab, Wiley Online Library on [29/01/2025]. See the Terms and Conditions (https://onlinelibrary.wiley.com/terms-and-conditions) on Wiley Online Library for rules of use; OA articles are governed by the applicable Creative Commons License

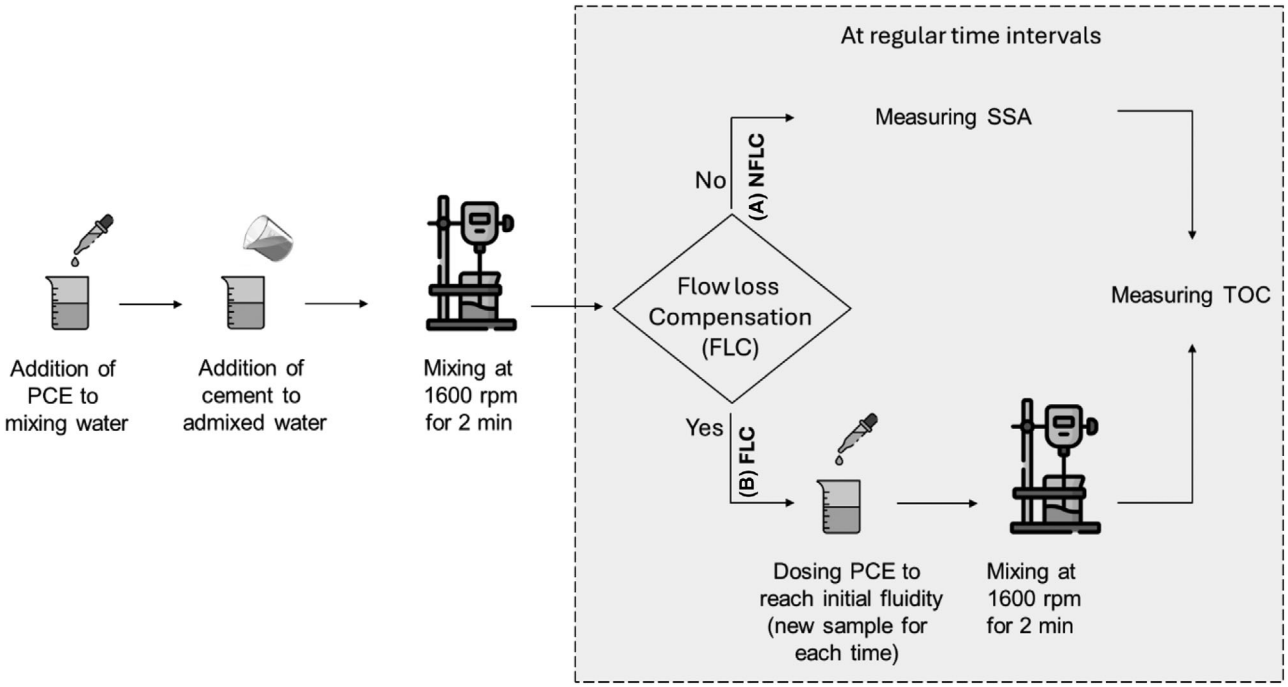

FIGURE 1 Schematic representation of experimental setup used in the study: (A) with no flow loss compensation (NFLC), and (B) with flow loss compensation (FLC).

then introduced to the solution for adsorption, mixed for 2 minutes, and allowed to rest for 5 minutes. After the rest period, a few grams of the paste were sampled for TOC analysis.

For the PCE adsorption experiments, samples were collected immediately after mixing and at regular 15-minute intervals, for both the cases of flow loss compensation and no flow loss compensation. In both experiments, the collected samples were centrifuged at 10,000 rpm for 10 min. The supernatant was carefully extracted, filtered through a 0.20 μm syringe filter, and diluted at least 20 times with 0.05 M HCl. The diluted solutions were analyzed using a TOC analyzer (TOC-V CSH, Shimadzu).[33]

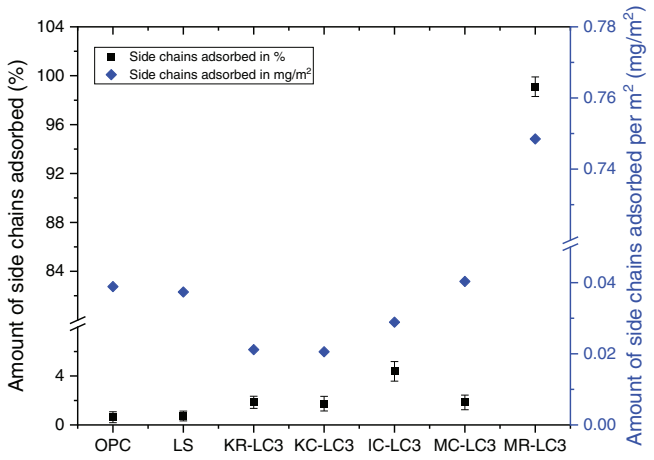

FIGURE 2 Percentage of side chains adsorbed across different systems.

3 | RESULTS

3.1 | Adsorption of side chains in different LC3s

The potential contribution of PCE side chain intercalation to slump loss in LC3 cements was assessed by evaluating the adsorption characteristics of various LC3 cements containing both raw and calcined clays as well as OPC and limestone. The percentage of side chains adsorbed by each system, along with their adsorption relative to their SSA, is depicted in Figure 2. As shown in that figure, OPC and LS exhibit minimal adsorption of PCE side chains, with values of 0.63% and 0.73%, respectively. These non-zero values are unexpected, as OPC and limestone surfaces should ideally show zero adsorption due to the absence of functional groups capable of interacting with the surfaces. The slight adsorption observed might be due to minor experimental inaccuracies rather than true surface interactions. In contrast, the LC3 variants, which incorporate raw and calcined kaolinite (KR-LC3 and KC-LC3), show slightly higher adsorption at 1.85% and 1.74%, respectively. These values however still indicate a low affinity of PCEs side chains for kaolinitic clays. Moreover, the LC3 variant with calcined montmorillonite (MC-LC3) also exhibited a

15512916, 0, Downloaded from https://ceramics.onlinelibrary.wiley.com/doi/10.1111/jace.20344 by Univ of California Lawrence Berkeley National Lab, Wiley Online Library on [29/01/2025]. See the Terms and Conditions (https://onlinelibrary.wiley.com/terms-and-conditions) on Wiley Online Library for rules of use; OA articles are governed by the applicable Creative Commons License

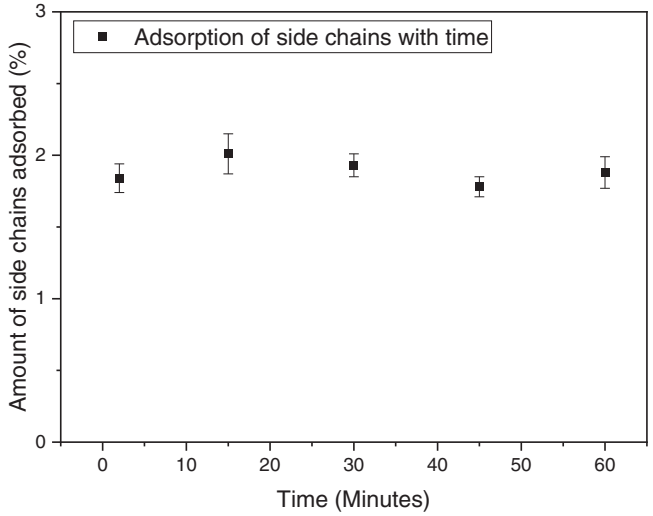

FIGURE 3 Adsorption behavior of side chains over time in LC3 with calcined montmorillonite (MC-LC3).

similar adsorption value of 1.84%, further indicating a low affinity for PCE side chains, even in the case of calcined montmorillonite. LC3 with industrially calcined clay (IC-LC3), on the other hand, exhibits a higher adsorption value of 4.38%, which can be attributed to its significantly high SSA, increasing their interaction with PCE side chains. This is evident as all systems, except MR-LC3, show similar adsorption values ranging between 0.02 and 0.04 mg/m^2.

However, the behavior of MR-LC3 is notably different. It displays exceptionally high adsorption at 99.1%, which contrasts sharply with the much lower values seen in MC-LC3. This significant difference highlights the fact that calcinating montmorillonite drastically reduces its ability to intercalate side chains.[40–42] Despite MC-LC3 representing the worst-case scenario for intercalation, the adsorption values remain very low, reinforcing that intercalation of PCE side chains is not a significant factor contributing to fluidity loss in LC3 systems.

While the above conclusions appear solid, there remains an important point often raised in the literature based on the behavior of PCEs in presence of non-calcined swelling clays. Indeed, in such cases, PCEs adsorb strongly on the clays owing to a strong affinity of their side chains for intercalation between such clays.[22,43,44] This raises the question of whether such a process may be slowly activated overtime with calcined clays after contact with water. To address this concern, the adsorption behavior of LC3 with calcined montmorillonite (MC-LC3) over time was analyzed and is presented in Figure 3. The results clearly show that adsorption does not change within the first hour, further reinforcing the conclusion that PCE intercalation is not responsible for rapid slump loss in superplasticizer LC3 cements. The consistently low adsorption values observed across all LC3 cements containing calcined clays, particularly in formulations predominantly using kaolinitic clays, indicate that intercalation of PCE side chains cannot account for the observed slump loss. The level of interaction is insufficient to cause significant fluidity reduction. These findings suggest that other mechanisms, rather than PCE intercalation, are responsible for the slump loss observed in superplasticized LC3 systems.

3.2 | Role of calcined clays in early hydration reactions

Since the results from the previous section confirm that PCE side chain intercalation is not responsible for the slump loss observed in LC3 systems, we now turn to explore other factors that may cause this rapid slump loss. The impact of hydration behavior and surface area development, which are critical for workability of any cementitious system, is investigated next. To further understand these aspects, the hydration behavior and surface area development of two LC3 systems—KR-LC3 (containing raw clay) and KC-LC3 (containing calcined clay)—were analyzed. Heat flow data provides insight into the differences in hydration between these two systems. In Figure 4A, which focuses on the initial 2 h of hydration, both LC3 formulations show a pronounced exothermic peak, pointing to a rapid release of heat due to dissolution of soluble phases. KC-LC3 exhibits a slightly higher peak heat flow compared to KR-LC3, and its heat rate and cumulative heat remains slightly higher throughout the first 2 hours indicating a more vigorous dissolution with the calcined clay. Figure 4B, which spans 48 hours, shows that the hydration rate and cumulative heat in KC-LC3 remain consistently higher. The alite peak in KC-LC3 occurs slightly earlier and with marginally higher intensity compared to KR-LC3, suggesting a slight acceleration in the main peak.

As shown in Figure 5, initially both systems—LC3 with raw clay (KR-LC3) and calcined clay (KC-LC3)—exhibit similar specific surface areas (SSAs), with KR-LC3 at 4.7 m^2/g and KC-LC3 at 4.3 m^2/g. By the end of the observation period, KR-LC3 shows only a moderate increase in SSA, reaching 5.3 m^2/g, indicating limited changes when raw clay is present. In contrast, KC-LC3 demonstrates a significant increase in SSA, rising to 6.0 m^2/g, despite starting with a lower initial SSA (4.3 m^2/g) than KR-LC3, as a consequence of more active dissolution and consequent enhanced precipitation of hydrates. This substantial increase could have different origins:

1. There could be a filler effect, which enhances the dissolution of cement phases and the precipitations of

15512916, 0, Downloaded from https://ceramics.onlinelibrary.wiley.com/doi/10.1111/jace.20344 by Univ of California Lawrence Berkeley National Lab, Wiley Online Library on [29/01/2025]. See the Terms and Conditions (https://onlinelibrary.wiley.com/terms-and-conditions) on Wiley Online Library for rules of use; OA articles are governed by the applicable Creative Commons License

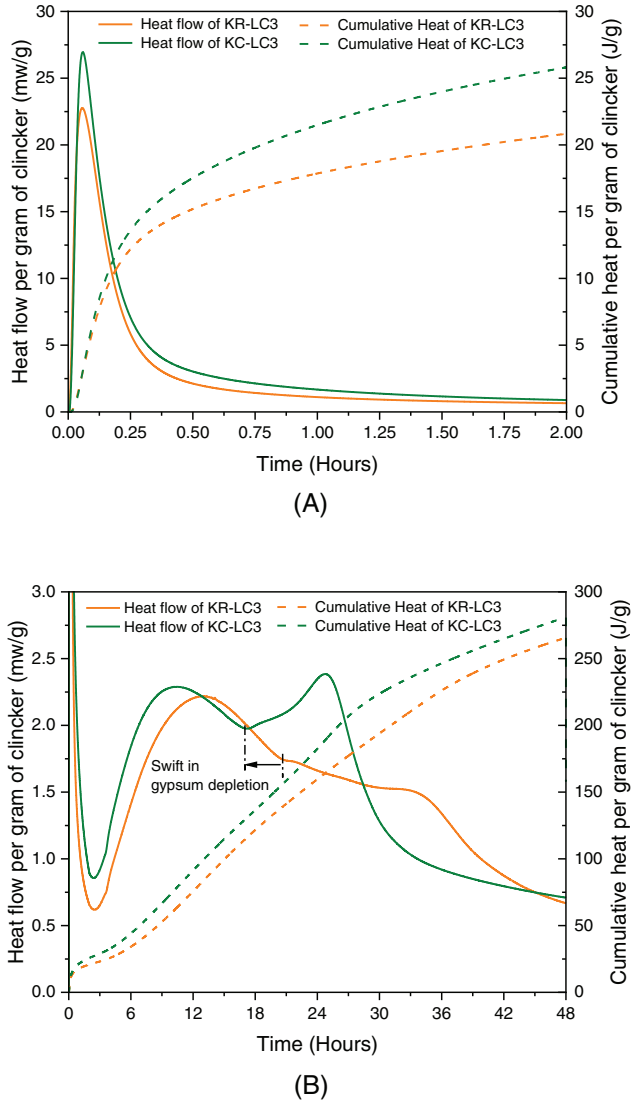

FIGURE 4 Heat flow of LC3 variants with raw and calcined clays (KR-LC3 and KC-LC3): (A) over 2 h, and (B) over 48 h.

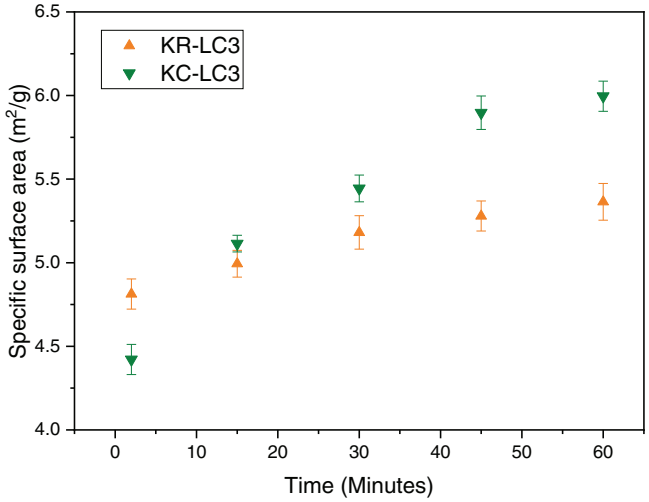

FIGURE 5 Time evolution of SSA for LC3 variants with raw and calcined clays (KR-LC3 and KC-LC3).

hydration products in LC3 with calcined clays, possibly enhanced due to altered surface energetics.[45]

2. The amorphous nature of calcined clay, with increased structural disorder, provides more reactive sites through the dissolution of clay minerals even at early hours of hydration.[46,47]

To understand the contribution of calcined clays, different model systems have been proposed.[34,46,48] As any model system they have their advantages and limitations. Their key feature is to eliminate the need for using OPC and limestone, leading to systems to study with different clays which helps to see reactions that may be masked by other exothermic reactions of cement phases. However, the limitation is the lack of competition between different phases of OPC, which in turn can yield significantly different dissolution kinetics. This paper reports model system from Scherb et al.[34]

For that model system, Figure 6A, which focuses on early hydration shows that calcined clay (KCC) has a higher heat flow rate, indicating better dissolution of the calcined clay. In contrast, the model system with raw clay (KRC) shows an initial low heat flow that drops sharply, suggesting that the observed heat is primarily due to mixing, with little contribution from clay dissolution. Figure 6B, which extends to 48 hours, reveals that the heat flow in the KRC system continues to rise even after a dormant period, reaching its first peak between 18 and 24 hours. This peak is attributed to the formation of ettringite and calcium aluminosilicate hydrates (C–A–S–H) due to the reaction between calcined clay, calcium hydroxide, and calcium sulfate, with additional peaks occurring between 24 and 36 hours. For a more detailed interpretation of these curves, refer to Scherb et al.[34]

It could be inferred from the model system that the shift in gypsum depletion point and slight acceleration in KC-LC3 might be due to the early reaction of metakaolin, which promotes the formation of ettringite and C–A–S–H, consuming calcium hydroxide and gypsum more rapidly. However, this hypothesis warrants further investigation for confirmation. Moreover, previous studies looking at the early phase assemblage of LC3 cements have found no evidence of an increase amount of ettringite formation during the induction and acceleration period, although LC3 systems still exhibit a higher amount of ettringite per gram of binder compared to OPC systems during the early periods.[48–51] Collectively, these findings suggest that calcined clays are indeed contributing to the development of surface area at early age, leading to fast slump loss although, the underlying mechanism deserves further investigation.

15512916, 0, Downloaded from https://ceramics.onlinelibrary.wiley.com/doi/10.1111/jace.20344 by Univ of California Lawrence Berkeley National Lab, Wiley Online Library on [29/01/2025]. See the Terms and Conditions (https://onlinelibrary.wiley.com/terms-and-conditions) on Wiley Online Library for rules of use; OA articles are governed by the applicable Creative Commons License

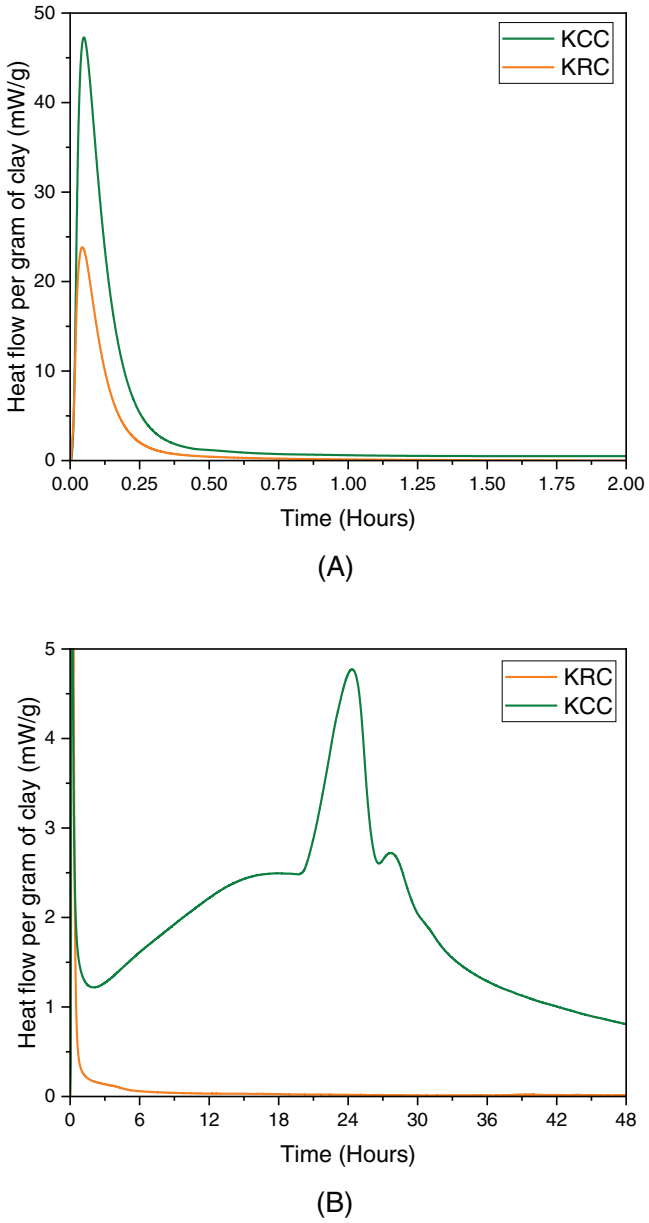

FIGURE 6 Heat flow of model systems with raw and calcined clay (kaolinitic raw clay (KRC) and kaolinitic calcined clay (KCC)): (A) over 2 h, and (B) over 48 h.

3.3 | Role of calcined clays in slump loss of LC3

The previous section clearly demonstrated that calcined clays enhance early hydration and surface area development in LC3 systems. Building on this, and to further elucidate the inability of superplasticizers to maintain workability, this section examines the adsorption of PCE in OPC and IC-LC3 systems as SSA increases. Figure 7 shows the evolution of SSA with time for OPC and IC-LC3 systems, where PCE was added only to the mixing water and no flow loss compensation (NFLC) was applied, labeled as OPC-NFLC and IC-LC3-NLFC, respectively. It is evident that IC-LC3 exhibits a faster increase in SSA over time compared to OPC (3.0 $m^2/g/h$ vs. 0.65 $m^2/g/h$), which can be attributed to the contribution of calcined clay in the early hydration reactions, leading to a higher SSA as time progresses.

In Figure 8, the adsorption of PCE is tracked over time for OPC and IC-LC3 with no flow loss compensation, and IC-LC3 with addition of PCE for flow loss compensation (IC-LC3-FLC). In the case of OPC-NFLC, as hydration progresses, PCE adsorption increases, indicating that PCE is adsorbing onto newly formed surfaces, such as C–A–S–H and ettringite. Despite no flow loss compensation, fluidity is maintained in the OPC system because the initial dosage provides sufficient PCE to adsorb onto the generated surfaces and effectively disperse the particles throughout the first 1 h of hydration.

For LC3 with no flow loss compensation (IC-LC3-NFLC), the adsorption remains stable over time with only a marginal increase, indicating that most of the superplasticizer is adsorbed early on, leaving little PCE available for later adsorption. Given that LC3 generates significantly more surfaces compared to OPC during early hydration, the lack of available PCE results in insufficient dispersion of the newly generated surfaces, which explains the fluidity loss over time. When that loss in fluidity is compensated by adding PCE (IC-LC3-FLC) at different times, adsorption increases as expected. More importantly, it can be expected that this additional adsorption must allow the complete dispersion of the newly formed surfaces.

4 | DISCUSSION

The results from Sections 3.1 and 3.2 indicate that PCE side chain intercalation does not significantly contribute to slump loss in LC3 systems, and that calcined clays enhance early hydration and surface area development. These findings are robust and do not require further analysis. The following discussion therefore focuses on Section 3.3, specifically analyzing how, over time, changes in SSA and PCE adsorption account for the observed slump loss in LC3 systems.

4.1 | Relation between PCE adsorption and surface area changes

From Figures 7 and 8, it appears that both SSA and PCE adsorption increase linearly with time up to about 1 hour. A linear regression is therefore taken over this linear range to infer the values of both SSA and adsorption at time zero, just as the cement is contacted with water. With this

15512916, 0, Downloaded from https://ceramics.onlinelibrary.wiley.com/doi/10.1111/jace.20344 by Univ of California Lawrence Berkeley National Lab, Wiley Online Library on [29/01/2025]. See the Terms and Conditions (https://onlinelibrary.wiley.com/terms-and-conditions) on Wiley Online Library for rules of use; OA articles are governed by the applicable Creative Commons License

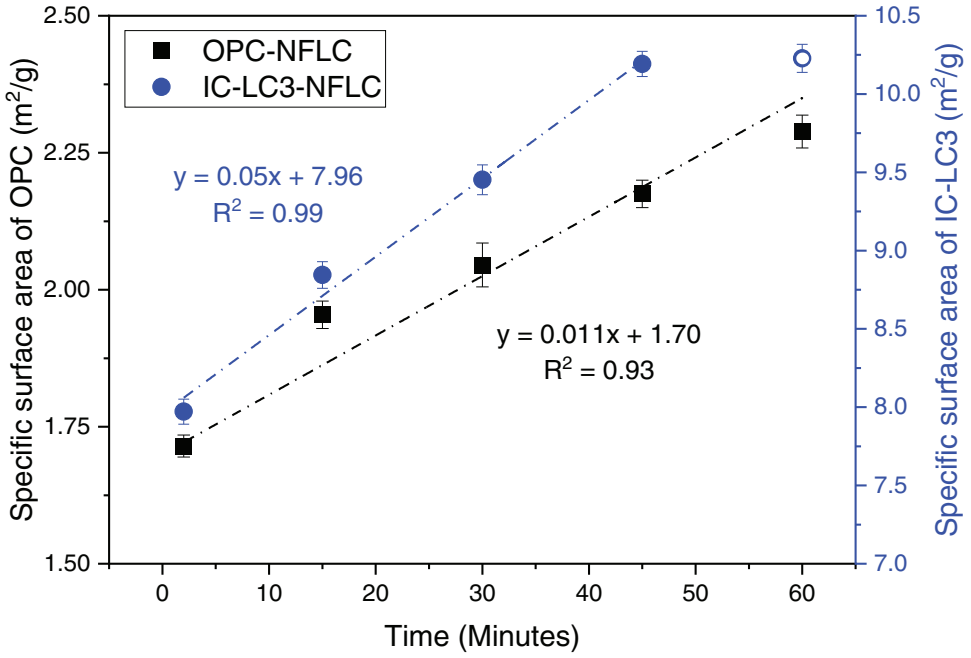

FIGURE 7 Time evolution of SSA for (OPC and IC-LC3 (LC3 with industrially calcined clay) with no flow loss compensation (NFLC). The rate at which SSA is forming in OPC and IC-LC3 is respectively, 3.0 $m^2/g/min$ and 0.65 $m^2/g/h$.

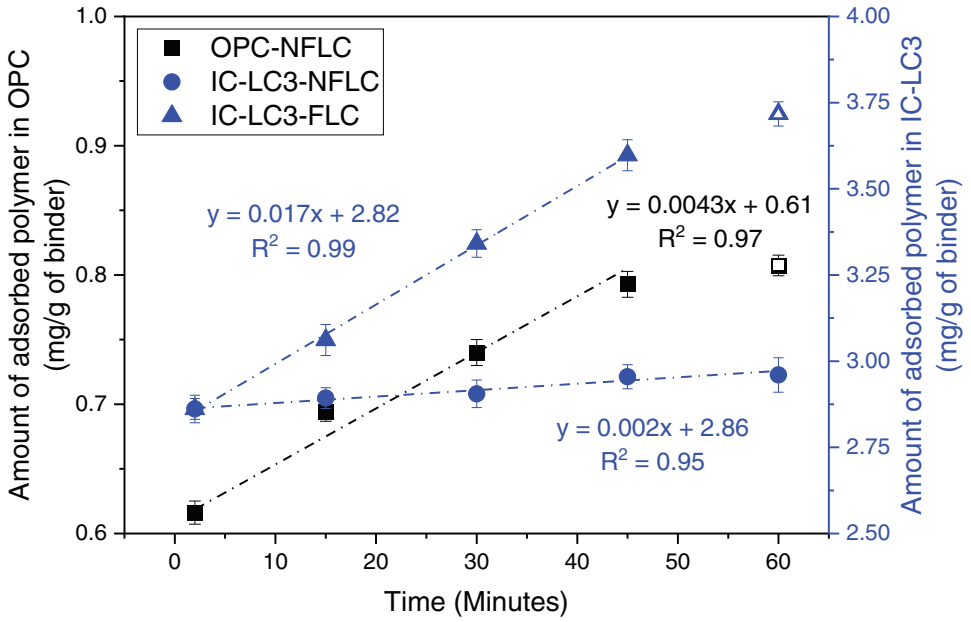

FIGURE 8 Adsorption of PCE over time in OPC with no flow loss compensation (NFLC), and in IC-LC3 (LC3 with industrially calcined clay) with flow loss compensation (FLC).

in hand, we calculate changes in both SSA (ΔSSA) and adsorption (ΔAds), starting from time zero.

Figure 9 shows that ΔAds increases linearly with ΔSSA in the three cases considered. However, for LC3 without flow loss compensation (LC3, circles), this increase is only minimal. This is in line with our previous conclusion, that with LC3 most of the dosed PCE adsorbs initially (> 75%). It points to the fact that the additionally formed surfaces strengthen the cohesion between grains, causing an increase in yield stress, explaining the rapid flow loss in superplasticized LC3.

The other two cases in Figure 9 show a much stronger increase of ΔAds with ΔSSA. Let us first consider the case of LC3 with flow compensation (LC3-FLC, triangles). As a

15512916, 0, Downloaded from https://ceramics.onlinelibrary.wiley.com/doi/10.1111/jace.20344 by Univ of California Lawrence Berkeley National Lab, Wiley Online Library on [29/01/2025]. See the Terms and Conditions (https://onlinelibrary.wiley.com/terms-and-conditions) on Wiley Online Library for rules of use; OA articles are governed by the applicable Creative Commons License

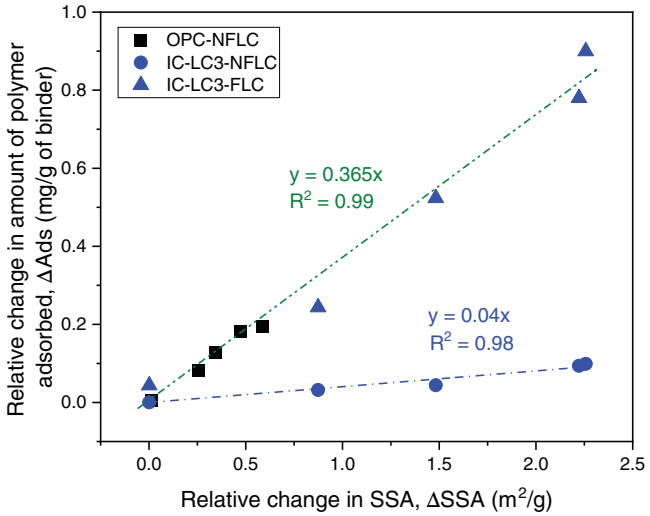

FIGURE 9 Relationship between the changes in polymer adsorption and SSA. Values are calculated by taking adsorption and SSA values at time zero from the ordinates at the origin of the regressions in Figures 7 and 8.

reminder, these data are obtained from samples to which, at each selected time, enough PCE is added to restore the initial fluidity. Figure 8 shows that this flow loss compensation fluidity goes along with an increase adsorption, ΔAds, that is proportional to ΔSSA. In other words, if enough PCE can adsorb on these additional surfaces, then the flow is retained. Returning to the normal case of LC3 without flow loss compensation, this underlines that rapid flow loss of superplasticized LC3 is a result of ΔSSA.

The last case in Figure 9 is that of OPC. Interestingly, it shows an equivalent proportionality between ΔAds and ΔSSA, with fluidity being retained although no additional PCE needs to be added over time. A first implication of this result is that in essence the mechanism of flow loss in OPC is the same as that in LC3: the creation of new surfaces that increase the cohesion of the flocculated network. Additionally, it also implies that retaining fluidity requires enough PCEs to adsorb on those freshly created surfaces.

The two main differences between OPC and LC3 are: (1) the rate at which these additional surfaces are formed (3.0 $m^2/g/h$ vs. 0.65 $m^2/g/h$), (2) Not all PCE initially adsorbed on OPC, contrary to LC3. Regarding the second point, we find that initial adsorption on OPC only concerns about 52% of the dosed polymer, while for LC3 it is much higher (75%).

This difference in adsorption can be attributed to the distribution of molecular structures in PCEs, particularly with regard to charge density, which has a profound effect on the affinity of PCEs for surfaces. We therefore infer that the low charge density part of the PCE distribution cannot initially adsorb on OPC, while it can on LC3. Despite this, over time and in OPC, this lower charge density fraction progressively adsorbs as SSA increases.

This suggests that PCEs have a higher affinity for these newly formed surfaces than for the original OPC. Also, since most PCE adsorbs on LC3 during flow compensation, one may suspect that the newly formed surfaces are of similar nature both in LC3 and in OPC, but this clearly deserves further investigation. In any case, regarding LC3 which is the core topic of this paper, based on model systems of the type used in this paper, the additional surfaces formed appear to be ettringite and C–A–S–H.[50] For ettringite, PCEs are said to have a strong affinity, which would explain why most dosed PCEs adsorb.[52,53] This suggests that ettringite may also plays a key role in ΔSSA of OPC since the less charged PCEs are able to adsorb on the newly surfaces that form.

4.2 | Surface coverage of newly formed hydrates

The previous section suggests that as new surfaces are formed, they must be covered by PCEs to prevent flow loss. Also, the relation between ΔAds and ΔSSA is very similar for OPC and LC3-FLC. Assuming that the increased adsorption occurs on newly formed hydrates, the proportionality constant gives the surface coverage of those hydrates, which from Figure 9 would be 0.365 mg/m^2. Should these surfaces be fully covered, we may compare that previous value to the theoretically expected saturation plateau obtained from an adsorption conformation model described elsewhere.[54]

The maximum adsorbed mass of PCE (m_∞) is given by:

$$m_\infty = \frac{M_w \times 1000}{S_{PCE} \times N_a}$$

where, M_w is the molar mass in g/mol, N_a is the Avogadro's number and S_{PCE} is the surface area occupied by a PCE molecule, calculated using:

$$S_{PCE} = \frac{\pi}{\sqrt{2}}(a_P a_N)\left(2\sqrt{2}(1-2\chi)\frac{a_P}{a_N}\right)^{2/5} P^{9/10} N^{3/10} n$$

where, a_N is the monomer size of the backbone (0.25 nm for methacrylate); a_P is the monomer size of the side chain (0.36 nm for ethylene oxide); χ is the Flory parameter (0.37 for polyethylene oxide at 25°C[55]); N is the number of monomers in the backbone between any two successive side chains; P is the number of monomers per side chain and n is the number of repeating structural units in the backbone.[56]

15512916, 0, Downloaded from https://ceramics.onlinelibrary.wiley.com/doi/10.1111/jace.20344 by Univ of California Lawrence Berkeley National Lab, Wiley Online Library on [29/01/2025]. See the Terms and Conditions (https://onlinelibrary.wiley.com/terms-and-conditions) on Wiley Online Library for rules of use; OA articles are governed by the applicable Creative Commons License

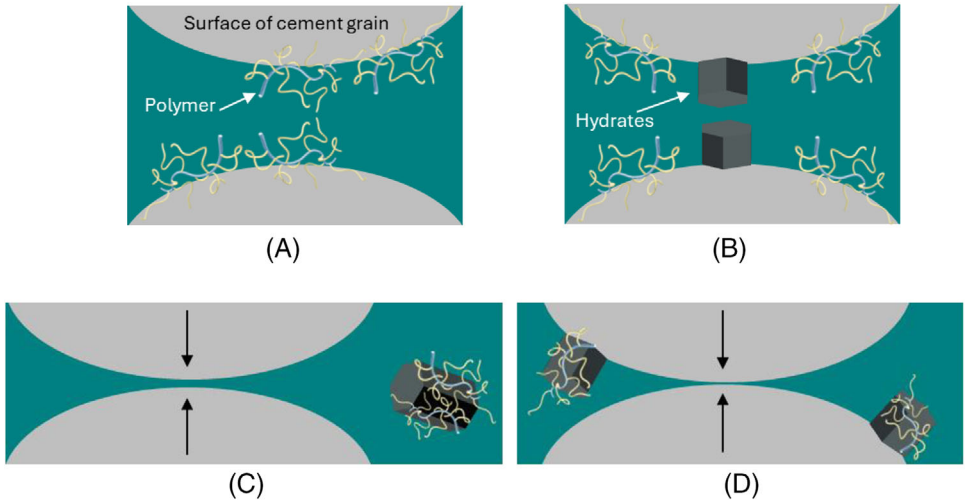

FIGURE 10 Highly schematic representation of possible causes for the evolution of yield stress in PCE superplasticized suspensions: (A) flocculated network with superplasticizer distribution, (B) strengthening of contact points from hydrate precipitation, (C) superplasticizer migration toward newly formed hydrates in the bulk and closer cement particles, and (D) migration of superplasticizer onto newly formed surfaces and cement particles moving closer.

Using these equations, the value of m_∞ was calculated as 0.375 mg/m^2. However, it was noted that the theoretical surface areas are typically 13% higher than experimental values.[54] After applying this correction, the adjusted value becomes 0.326 mg/m^2, which still closely matches the experimentally obtained value of 0.365 mg/m^2, suggesting that PCEs not only adsorbs onto new surfaces generated, but also cover them extensively.

4.3 | Microscopic look at flow loss and its compensation

As explained in the introduction, the yield stress of superplasticized suspensions may change due to the precipitation of hydrates, which strengthens the flocculated network of particles. Superplasticizers, however, substantially reduce the strength of any contact where they are present. Therefore, adding hydrates at contact points and not covering them with superplasticizers will substantially increase the yield stress. This situation is illustrated in Figure 10A,B. The first of those illustrations shows two particles with a low contact strength because superplasticizers are present at their point of closest vicinity. Figure 10B then shows the same particles with the formation of hydrates that strength the interparticle cohesion. That illustration includes a change of position of some PCEs which reflects the fact that adsorbed polymers remain mobile, which is indirectly supported by experimental evidence that PCE adsorption is reversible.[33,57]

Figure 10C shows a newly formed hydrate in the bulk and PCEs having migrated from the cement grains to its surface. This leads both cement particles to come closer together and have stronger cohesive forces, without additional hydrates having to form on their surface.

The fourth illustration shown as Figure 10D is a combination of cases (B) and (C). Here hydrates are forming on the cement grains, but they are not directly causing an increase in interparticle cohesion, because PCEs migrate to their surface. The change in cohesion comes from parts of the original surface now being devoid of PCEs.

While the situations illustrated in Figure 10B–D would have the same macroscopic consequence on yield stress and flow loss, they are not completely equivalent in terms of the affinity that the PCE must have for those surfaces as explained in Appendix A, which also elaborates on the role of PCE dispersity.

4.4 | Strategies for mitigating flow loss in LC3

The root cause for the faster flow loss in LC3 than in OPC is the faster rate at which additional surfaces are created (3.0 m^2/g/h vs. 0.65 m^2/g/h). This implies that two main strategies may be considered to counter that flow loss.

The first one would be to include poorly adsorbing substances that would not adsorb initially but only later in time as additional surface are formed. This would mimic the situation observed with our PCE in OPC but may be more difficult to achieve as LC3 seems to attract PCEs more than OPC. A more fundamental issue with this option is that it does not tackle the root cause of substantial increase in SSA over time.

15512916, 0, Downloaded from https://ceramics.onlinelibrary.wiley.com/doi/10.1111/jace.20344 by Univ of California Lawrence Berkeley National Lab, Wiley Online Library on [29/01/2025]. See the Terms and Conditions (https://onlinelibrary.wiley.com/terms-and-conditions) on Wiley Online Library for rules of use; OA articles are governed by the applicable Creative Commons License

Consequently, the needed dosages of PCEs will increase substantially.

A more promising route to prevent flow loss of superplasticized LC3, and one already reported to be effective, is to use additional admixtures that hinder the early reactivity of LC3, such as diphosphonate superplasticizers.[14] Other studies however reported the use of clay-mitigating agents[58] and clay-dispersing agents[59] which probably also impact the early hydration of LC3, limiting the formation of additional surfaces. While this provides a clear conceptual route to control flow loss in superplasticized LC3, the underlying chemistry and physics deserve additional research, particularly in terms of molecular design of such additives or formulations in relation to the early reactivity of calcined clays.

5 | CONCLUSIONS

This research delves into the underlying causes of slump loss in superplasticized LC3, emphasizing the impact of calcined clays and their interaction with PCEs. Our findings provide critical insights into the mechanisms driving fluidity loss not only in LC3 but also systems and offer potential pathways for improving workability.

Our key conclusions can be summarized as follows:

1. Calcined clays and early hydration: Calcined kaolinitic clays significantly contribute to the increase in SSA and influence the hydration process. This increased SSA is a key factor in the observed slump loss in superplasticized LC3.
2. PCE interaction and fluidity: The use of a single PCE molecule, as in this study, is insufficient to manage slump loss in LC3. The PCE's inability to maintain fluidity in LC3 is primarily due to its initial extensive adsorption, which leaves no reserve for adsorption over time as additional surfaces are created. Higher initial dosages are not an option as they would lead to too high fluidity, possibly with segregation and/or bleeding.
3. Intercalation of PCE side chains: Intercalation of PCE side chains into calcined clays, particularly montmorillonite, is not a significant factor in fluidity loss when those clays have been calcined. Even in montmorillonite clays, which represent a worst-case scenario, the adsorption values were too low to contribute meaningfully to slump loss.
4. Recommendations for improving slump retention: To effectively address slump loss in LC3, PCE formulations may need to be optimized or modified with different adsorbing groups. Alternatively, combining PCE with additives such as diphosphonates, as proposed in previous studies, could offer a tailored solution to meet the specific demands of slump retention in superplasticizer LC3 systems. Thereby, the most effective mechanism for such admixtures should be to hinder a too rapid initial reaction of the calcined clays.
5. Strategies for mitigating flow loss in LC3 and future research directions: Current strategies to mitigate flow loss in LC3 primarily involve using admixtures such as diphosphonate superplasticizers, clay-mitigating agents, and clay-dispersing agents. However, further research is needed to optimize the molecular design of PCEs to better control reactivity and surface generation, enhancing their compatibility with LC3.

ACKNOWLEDGMENTS

We gratefully acknowledge the funding provided to Sirajuddin Moghul by the Swiss National Science Foundation (SNF) under project no. 172481, titled "Functionally Diversified Superplasticizers for Sustainable Concrete." Dr. Franco Zunino was supported by the Swiss National Science Foundation (SNSF) through an Ambizione fellowship (grant no. 208719). We sincerely thank Dr. Anne Weckwerth (Sika) for generously supplying the sidechains and PCE superplasticizer.

ORCID

Sirajuddin Moghul https://orcid.org/0000-0002-6407-7651

Franco Zunino https://orcid.org/0000-0002-1895-2742

REFERENCES

1. Korczak K, Kochański M, Skoczkowski T. Mitigation options for decarbonization of the non-metallic minerals industry and their impacts on costs, energy consumption and GHG emissions in the EU—systematic literature review. J Cleaner Prod. 2022;358:132006. https://doi.org/10.1016/j.jclepro.2022.132006
2. Juenger MCG, Winnefeld F, Provis JL, Ideker JH. Advances in alternative cementitious binders. Cem Concr Res. 2011;41(12):1232–43. https://doi.org/10.1016/j.cemconres.2010.11.012
3. Zunino F, Martirena F, Scrivener K. Limestone calcined clay cements (LC3). ACI Mater J. 2021;118(3). https://doi.org/10.14359/51730422
4. Scrivener K, Martirena F, Bishnoi S, Maity S. Calcined clay limestone cements (LC3). Cem Concr Res. 2018;114:49–56. https://doi.org/10.1016/j.cemconres.2017.08.017
5. Scrivener KL, John VM, Gartner EM. Eco-efficient cements: Potential economically viable solutions for a low-CO_2 cement-based materials industry. Cem Concr Res. 2018;114:2–26. https://doi.org/10.1016/j.cemconres.2018.03.015
6. Ito A, Wagai R. Global distribution of clay-size minerals on land surface for biogeochemical and climatological studies. Sci Data. 2017;4(1):170103. https://doi.org/10.1038/sdata.2017.103
7. Antoni M, Rossen J, Martirena F, Scrivener K. Cement substitution by a combination of metakaolin and limestone.

15512916, 0, Downloaded from https://ceramics.onlinelibrary.wiley.com/doi/10.1111/jace.20344 by Univ of California Lawrence Berkeley National Lab, Wiley Online Library on [29/01/2025]. See the Terms and Conditions (https://onlinelibrary.wiley.com/terms-and-conditions) on Wiley Online Library for rules of use; OA articles are governed by the applicable Creative Commons License

Cem Concr Res. 2012;42(12):1579–89. https://doi.org/10.1016/j.cemconres.2012.09.006
8. Scrivener K, Avet F, Maraghechi H, Zunino F, Ston J, Hanpongpun W, et al. Impacting factors and properties of limestone calcined clay cements (LC^3). Green Mater. 2019;7(1):3–14. https://doi.org/10.1680/jgrma.18.00029
9. Zunino F. A two-fold strategy towards low-carbon concrete. RILEM Tech Lett. 2023;8:45–58. https://doi.org/10.21809/rilemtechlett.2023.179
10. Nair N, Mohammed Haneefa K, Santhanam M, Gettu R. A study on fresh properties of limestone calcined clay blended cementitious systems. Constr Build Mater. 2020;254:119326. https://doi.org/10.1016/j.conbuildmat.2020.119326
11. Schmid M, Plank J. Dispersing performance of different kinds of polycarboxylate (PCE) superplasticizers in cement blended with a calcined clay. Constr Build Mater. 2020;258:119576. https://doi.org/10.1016/j.conbuildmat.2020.119576
12. Muzenda TR, Hou P, Kawashima S, Sui T, Cheng X. The role of limestone and calcined clay on the rheological properties of LC3. Cem Concr Compos. 2020;107:103516. https://doi.org/10.1016/j.cemconcomp.2020.103516
13. Chen Y, Zhang Y, He S, Liang M, Zhang Y, Schlangen E, et al. Rheology control of limestone calcined clay cement pastes by modifying the content of fine-grained metakaolin. J Sustainable Cement-Based Mater. 2023;12(9):1126–40. https://doi.org/10.1080/21650373.2023.2169965
14. Moghul S, Sreeram S, Sha S, Zunino F, Flatt RJ. Combined effect of polycarboxylate ether and phosphonated superplasticizers in limestone calcined clay cement. *SP-362: ICCM2024*. Michigan: American Concrete Institute; 2024 https://doi.org/10.14359/51741004
15. Favier A, Zunino F, Katrantzis I, Scrivener K. The Effect of Limestone on the Performance of Ternary Blended Cement LC3: Limestone, Calcined Clays and Cement. In: Martirena F, Favier A, Scrivener K, editors. Calcined clays for sustainable concrete. Dordrecht, Netherlands: Springer; 2018. p. 170–5.
16. Hou P, Muzenda TR, Li Q, Chen H, Kawashima S, Sui T, et al. Mechanisms dominating thixotropy in limestone calcined clay cement (LC3). Cem Concr Res. 2021;140:106316. https://doi.org/10.1016/j.cemconres.2020.106316
17. Ng S, Justnes H. Influence of dispersing agents on the rheology and early heat of hydration of blended cements with high loading of calcined marl. Cem Concr Compos. 2015;60:123–34. https://doi.org/10.1016/j.cemconcomp.2015.04.007
18. Michel L, Zunino F, Flatt RJ, Kammer DS. Early-age workability loss in LC3 systems. In: Further reduction of CO_2-emissions and circularity in the cement and concrete industry. Bangkok: Thailand Concrete Association; 2023. p. 43–6. https://doi.org/10.3929/ETHZ-B-000644519
19. Vikan H, Justnes H. Rheology of cementitious paste with silica fume or limestone. Cem Concr Res. 2007;37(11):1512–7. https://doi.org/10.1016/j.cemconres.2007.08.012
20. Yahia A, Tanimura M, Shimoyama Y. Rheological properties of highly flowable mortar containing limestone filler-effect of powder content and W/C ratio. Cem Concr Res. 2005;35(3):532–9. https://doi.org/10.1016/j.cemconres.2004.05.008
21. Nkinamubanzi P-C, Mantellato S, Flatt RJ. Superplasticizers in practice. In: Science and technology of concrete admixtures. New York: Elsevier; 2016. p. 353–77. https://doi.org/10.1016/B978-0-08-100693-1.00016-3
22. Ng S, Plank J. Interaction mechanisms between Na montmorillonite clay and MPEG-based polycarboxylate superplasticizers. Cem Concr Res. 2012;42(6):847–54. https://doi.org/10.1016/j.cemconres.2012.03.005
23. Lei L, Plank J. A study on the impact of different clay minerals on the dispersing force of conventional and modified vinyl ether based polycarboxylate superplasticizers. Cem Concr Res. 2014;60:1–10. https://doi.org/10.1016/j.cemconres.2014.02.009
24. Borralleras P, Segura I, Aranda MAG, Aguado A. Absorption conformations in the intercalation process of polycarboxylate ether based superplasticizers into montmorillonite clay. Constr Build Mater. 2020;236:116657. https://doi.org/10.1016/j.conbuildmat.2019.08.038
25. Mantellato S, Palacios M, Flatt RJ. Relating early hydration, specific surface and flow loss of cement pastes. Mater Struct. 2019;52(1):5. https://doi.org/10.1617/s11527-018-1304-y
26. Michel L. Structural build-up at rest in the induction and acceleration periods of Portland cement. Cem Concr Res. 2024;186:107665.
27. Sha S, Mantellato S, Weckwerth SA, Zhang Z, Shi C, Flatt RJ. Do superplasticizers work the way we think? New insights from their effect on the percolation threshold of limestone pastes. Cem Concr Res. 2023;172:107235. https://doi.org/10.1016/j.cemconres.2023.107235
28. Flatt RJ, Roussel N, Bessaies-Bey H, Caneda-Martínez L, Palacios M, Zunino F. From physics to chemistry of fresh blended cements. Cem Concr Res. 2023;172:107243. https://doi.org/10.1016/j.cemconres.2023.107243
29. Fernández R, Scrivener K. In: Faculté Sciences et Techniques de L'Ingeniur PhD Thesis Laboratory of Construction Materials École Polytechnique Federale de Lausanne: Lausanne. 2009;1–178.
30. Zunino F, Scrivener K. The influence of the filler effect on the sulfate requirement of blended cements. Cem Concr Res. 2019;126:105918. https://doi.org/10.1016/j.cemconres.2019.105918
31. Perrot A, Lecompte T, Khelifi H, Brumaud C, Hot J, Roussel N. Yield stress and bleeding of fresh cement pastes. Cem Concr Res. 2012;42(7):937–44. https://doi.org/10.1016/j.cemconres.2012.03.015
32. Shetty A, Goyal A. Total organic carbon analysis in water—a review of current methods. Mater Today: Proc. 2022;65:3881–6. https://doi.org/10.1016/j.matpr.2022.07.173
33. Weckwerth SA, Temme RL, Flatt RJ. Experimental method and thermodynamic model for competitive adsorption between polycarboxylate comb copolymers. Cem Concr Res. 2022;151:106523. https://doi.org/10.1016/j.cemconres.2021.106523
34. Scherb S, Maier M, Beuntner N, Thienel K-C, Neubauer J. Reaction kinetics during early hydration of calcined phyllosilicates in clinker-free model systems. Cem Concr Res. 2021;143:106382. https://doi.org/10.1016/j.cemconres.2021.106382
35. Pierre A. Applied Rheology. Extension of spread-slump formulae for yield stress evaluation. Berlin: De Gruyter; 2013. https://doi.org/10.3933/APPLRHEOL-23-63849
36. Mantellato S, Palacios M, Flatt RJ. Impact of sample preparation on the specific surface area of synthetic ettringite. Cem Concr

15512916, 0, Downloaded from https://ceramics.onlinelibrary.wiley.com/doi/10.1111/jace.20344 by Univ of California Lawrence Berkeley National Lab, Wiley Online Library on [29/01/2025]. See the Terms and Conditions (https://onlinelibrary.wiley.com/terms-and-conditions) on Wiley Online Library for rules of use; OA articles are governed by the applicable Creative Commons License

Res. 2016;86:20–8. https://doi.org/10.1016/j.cemconres.2016.04.005

37. Sha S, Sirajuddin M, Flatt RJ. D3 method: Direct and delayed dosing: new insights into specific surface area modification by superplasticizers. Cem Concr Res. 2024;181:107541. https://doi.org/10.1016/j.cemconres.2024.107541
38. Meier MR, Rinkenburger A, Plank J. Impact of different types of polycarboxylate superplasticisers on spontaneous crystallisation of ettringite. Adv Cem Res. 2016;28(5):310–9. https://doi.org/10.1680/jadcr.15.00114
39. Hathaway JC. Procedure for clay mineral analyses used in the sedimentary petrology laboratory of the U.S. geological survey. Clay Mineral Bull. 1956;3(15):8–13. https://doi.org/10.1180/claymin.1956.003.15.05
40. Bradley WF. Grim RE. High temperature thermal effects of clay and related materials. Am Mineralogist. 1951;36(3–4):182–201.
41. Brett NH, MacKenzie KJD, Sharp JH. The thermal decomposition of hydrous layer silicates and their related hydroxides. Q Rev Chem Soc. 1970;24(2):185. https://doi.org/10.1039/qr9702400185
42. Gu BX, Wang LM, Minc LD, Ewing RC. Temperature effects on the radiation stability and ion exchange capacity of smectites. J Nucl Mater. 2001.
43. Burchill S, Hall PL, Harrison R, Hayes MHB, Langford JI, Livingston WR, et al. Smectite-polymer interactions in aqueous systems. Clay Miner. 1983;18(4):373–97. https://doi.org/10.1180/claymin.1983.018.4.04
44. Ma Y, Shi C, Lei L, Sha S, Zhou B, Liu Y, et al. Research progress on polycarboxylate based superplasticizers with tolerance to clays—a review. Constr Build Mater. 2020;255:119386. https://doi.org/10.1016/j.conbuildmat.2020.119386
45. Zunino F, Palacios M, Bowen P, Scrivener K. Surface properties of clinker phases and clay minerals characterized by inverse gas chromatography (IGC) and their link to reactivity. Cem Concr Res. 2024;178:107458. https://doi.org/10.1016/j.cemconres.2024.107458
46. Demeusy Y, Gauffinet S, Labbez C. Rheology and early-age reactivity of calcined kaolinite. Am Conc Inst. 2024;686:610-4.
47. Fernandez R, Martirena F, Scrivener KL. The origin of the pozzolanic activity of calcined clay minerals: a comparison between kaolinite, illite and montmorillonite. Cem Concr Res. 2011;41(1):113–22. https://doi.org/10.1016/j.cemconres.2010.09.013
48. Maier M, Scherb S, Thienel K. Sulfate consumption during the hydration of Alite and its influence by SCMs. ce papers. 2023;6(6):2–7. https://doi.org/10.1002/cepa.2885
49. Zunino F, Scrivener K. Insights on the role of alumina content and the filler effect on the sulfate requirement of PC and blended cements. Cem Concr Res. 2022;160:106929. https://doi.org/10.1016/j.cemconres.2022.106929
50. Scherb S, Maier M, Beuntner N, Thienel K-C, Neubauer J. Reaction kinetics during early hydration of calcined phyllosilicates in clinker-free model systems. Cem Concr Res. 2021;143:106382. https://doi.org/10.1016/j.cemconres.2021.106382
51. Zunino F, Scrivener K. The influence of the filler effect on the sulfate requirement of blended cements. Cem Concr Res. 2019;126:105918. https://doi.org/10.1016/j.cemconres.2019.105918
52. Dalas F, Pourchet S, Rinaldi D, Nonat A, Sabio S, Mosquet M. Modification of the rate of formation and surface area of ettringite by polycarboxylate ether superplasticizers during early C3A–$CaSO_4$ hydration. Cem Concr Res. 2015;69:105–13. https://doi.org/10.1016/j.cemconres.2014.12.007
53. Plank J, Hirsch C. Impact of zeta potential of early cement hydration phases on superplasticizer adsorption. Cem Concr Res. 2007;37(4):537–42. https://doi.org/10.1016/j.cemconres.2007.01.007
54. Flatt RJ, Schober I, Raphael E, Plassard C, Lesniewska E. Conformation of adsorbed comb copolymer dispersants. Langmuir. 2009;25(2):845–55. https://doi.org/10.1021/la801410e
55. Stribeck N, Smarsly B. Scattering Methods and the Properties of Polymer Materials. Berlin, Heidelberg: Springer; 2005. https://doi.org/10.1007/b96538
56. Gay C, Raphaël E. Comb-like polymers inside nanoscale pores. Adv Colloid Interface Sci. 2001;94(1–3):229–36. https://doi.org/10.1016/S0001-8686(01)00062-8
57. Yamada K, Ogawa S, Hanehara S. Controlling of the adsorption and dispersing force of polycarboxylate-type superplasticizer by sulfate ion concentration in aqueous phase. Cem Concr Res. 2001;31(3):375–83. https://doi.org/10.1016/S0008-8846(00)00503-2
58. Ribeiro FRC, Silvestro L, Py LG, Sakata RD, Gleize PJP, Campos CEMd, et al. Assessing hydration kinetics and rheological properties of limestone calcined clay cement (LC3): influence of clay-mitigating and superplasticizer admixtures. Case Stud Constr Mater. 2024;20:e03364. https://doi.org/10.1016/j.cscm.2024.e03364
59. Bhattacherjee S, Jain S, Santhanam M. A method to increase the workability retention of concrete with limestone calcined clay based cementitious system using a dispersing agent containing sodium hexametaphosphate. Cem Conc Compos. 2022;132:104624. https://doi.org/10.1016/j.cemconcomp.2022.104624

How to cite this article: Moghul S, Zunino F, Flatt RJ. Flow loss in superplasticized limestone calcined clay cement. J Am Ceram Soc. 2024;e20344. https://doi.org/10.1111/jace.20344

Appendix A: Possible (re)distribution of PCEs on hydrates

The present paper has highlighted similar origins of flow loss for OPC and LC3, although the rate at which this happens is very different with both cements. One reason lies in the much higher rate of surface creation in LC3 than OPC than OPC (3.0 m^2/g/h vs. 0.65 m^2/g/h). Another reason results from the PCE polydispersity along with a lower affinity of our PCE for OPC than for LC3. To better illustrate this, we have developed the schemes in Figure A1.

OPC

Figure A1(A) illustrates the case of OPC, where the polyhedron represents a cement particle. Contacts between cement particles can be imagined as shown in Figure 10.

15512916, 0, Downloaded from https://ceramics.onlinelibrary.wiley.com/doi/10.1111/jace.20344 by Univ of California Lawrence Berkeley National Lab, Wiley Online Library on [29/01/2025]. See the Terms and Conditions (https://onlinelibrary.wiley.com/terms-and-conditions) on Wiley Online Library for rules of use; OA articles are governed by the applicable Creative Commons License

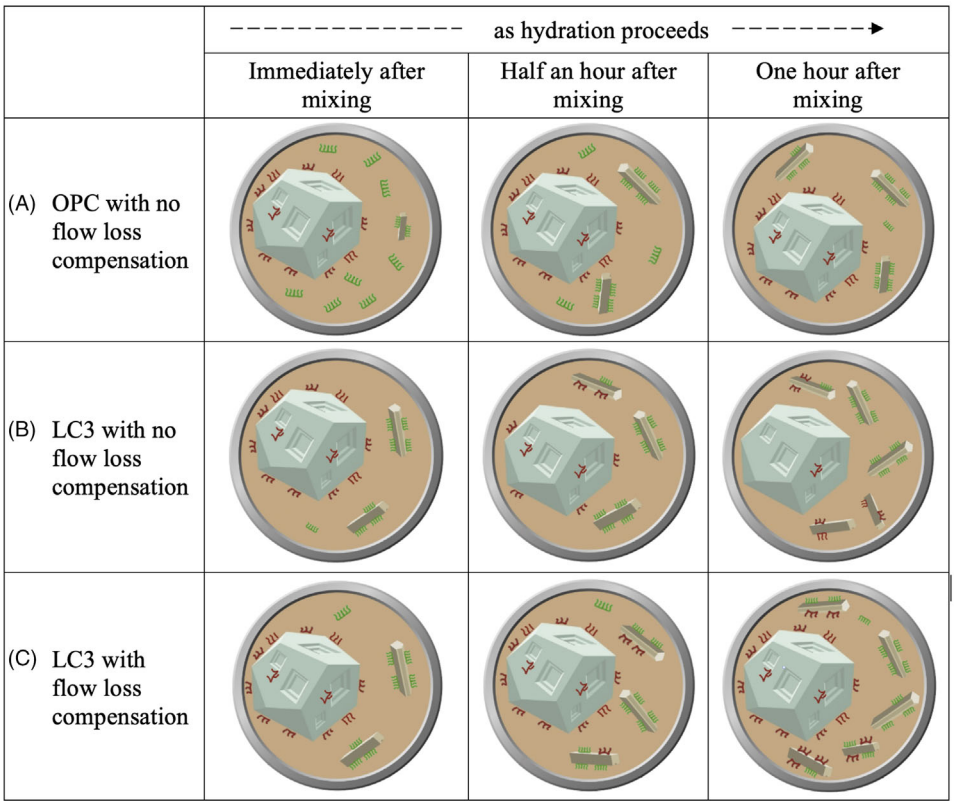

FIGURE A1 Visual representation of different systems over time, organized into rows and columns. The three rows represent different experimental setups: (A) Ordinary Portland cement (OPC) with no flow loss compensation (polycarboxylate ether superplasticizers (PCE) in the mixing water), (B) limestone calcined clay cement (LC3) with no flow loss compensation, and (C) LC3 with flow loss compensation (gradual addition of PCE at discrete time intervals). The three columns correspond to the adsorption of PCE at different hydration times: immediately after mixing, 30 min after mixing, and 1 h after mixing. PCE molecules are classified into two groups based on their charge density: low charge density (shown in green) and high charge density (shown in red). Cement particles are illustrated as polyhedrons, while ettringite is depicted as columnar structures. For simplicity, the new surfaces generated during hydration are shown as ettringite.

The columnar structures represent ettringite. The added PCE is broadly classified into two groups based on charge density: molecules with low charge density are represented in green, while those with high charge density are shown in red. The 2nd and 3rd illustration in this row show that over time additional surfaces form and absorb the previously non-adsorbed PCE. We speculate that whatever the hydrate forming (not necessarily ettringite or only it), PCEs have a higher affinity for it, so the lower charge density PCEs can adsorb onto those surfaces.

LC3 without flow loss compensation

In the case of LC3, most of the PCE is initially adsorbed, probably due to high SSA of LC3 and the fact that it forms more surfaces for which, as for ettringite, PCEs have a strong affinity. This implies that LC3 has little reserve PCE in solution to counter the effect of newly formed surfaces. Importantly also, because these surfaces cannot be covered by adsorbing PCEs, they will cause flow loss.[27,28] As already suggested in Figure 10, this process may also involve the new surface consuming the PCEs adsorbed on cement particles, thereby leading to hydrate bridges and flow loss. Whichever of those processes takes place, the result is a loss in fluidity. The scenario of hydrates forming in the bulk is the one shown in the 2nd and 3rd illustration of Figure A1(B) as it is easier to represent.

LC3 with flow loss compensation

Figure A1(C) shows the case where at selected points in time, an additional amount of PCE is added to return the fluidity to its initial value. As shown in Figure 9, this leads to an additional adsorption ΔAds that is proportional to ΔSSA. The analysis in Section 4.2 suggests that the additional surfaces are extensively covered by PCEs, indicating that they also attract lower charge density PCEs. The 2nd and 3rd illustrations of Figure A1(C) show the same formation of hydrates over time as in Figure A1(B), but this time with additional PCEs being made available to maintain an overall high surface coverage. This illustration should be considered along with Figure 10.

15512916, 0, Downloaded from https://ceramics.onlinelibrary.wiley.com/doi/10.1111/jace.20344 by Univ of California Lawrence Berkeley National Lab, Wiley Online Library on [29/01/2025]. See the Terms and Conditions (https://onlinelibrary.wiley.com/terms-and-conditions) on Wiley Online Library for rules of use; OA articles are governed by the applicable Creative Commons License